Infrared Spectroscopy of H-Bonded Bridges Stretched across the *cis*-Amide Group: II. Ammonia and Mixed Ammonia/Water Bridges

A. V. Fedorov and J. R. Cable*,†

Department of Chemistry and Center for Photochemical Sciences, Bowling Green State University, Bowling Green, Ohio 43403-0213

Joel R. Carney and Timothy S. Zwier*,‡

Department of Chemistry, Purdue University, West Lafayette, Indiana 47907-1393

Received: March 28, 2001; In Final Form: June 5, 2001

Clusters of two model *cis* amides, oxindole and 3,4-dihydro-2(1*H*)-quinolinone, containing one and two ammonia molecules have been studied in the IR hydride stretch region using resonant ion-dip IR spectroscopy. The spectra confirm that ammonia is able to form hydrogen-bonded bridges across the adjacent amide N−H and C═O sites in a manner very similar to that of water. Such bridged structures require that ammonia assume the role of a hydrogen bond donor. Further similarities of the hydrogen bonding capabilities of ammonia and water have been revealed by investigations of ternary clusters containing an amide, one ammonia, and one water molecule. Experimentally, two species are observed having IR spectra consistent with a hydrogen-bonded bridge structure. The two species differ only in the relative positions of the ammonia and water molecules within the bridge. These experimental results are well supported by optimized structures, vibrational frequencies, and IR intensities calculated using density functional theory with the Becke3LYP functional. Additionally, the characteristic features of the hydride stretch fundamentals in a hydrogen-bond-donating ammonia molecule can be readily understood using a simple model for the coupled NH oscillators in which the hydrogen-bonded NH has its force constant lowered and its dipole derivative increased, much like in other hydrogen-bonded XH groups.

I. Introduction

As a strong base, ammonia functions as a well-characterized hydrogen bond acceptor. However, hydrogen bonds in which ammonia serves as the donor are less common and hence not as well understood. The decreased polarity of the NH bonds and the 3-fold symmetry of the ammonia molecule produce weaker, less-directional hydrogen bonds that are often capable of large-amplitude motion. An extreme example of this is provided by the ammonia dimer, where structure determination has proven to be quite challenging due to the flatness of the potential energy surface and the low barriers to tunneling that accompany it. A recently obtained potential[1] that successfully reproduces the observed vibration-rotation-tunneling states and dipole moment[2] has an asymmetric cyclic equilibrium structure with a substantially nonlinear hydrogen bond and a barrier to donor−acceptor interchange of only 7 cm^{-1}. Recent high-level ab initio calculations estimate the electronic binding energy of the ammonia dimer to be 3.15 kcal/mol,[3] which is substantially less than that computed for the ammonia−water complex, 6.40 kcal/mol,[4] in which ammonia functions in its more conventional role as a hydrogen bond acceptor.

One approach that can be taken to force ammonia into a role as a hydrogen bond donor is to study complexes in which ammonia functions simultaneously as both a donor and an acceptor at two separate sites, forming a bridge between them. Notable examples of such ammonia-bridged complexes are those involving the *cis* amide 2-pyridone (2-PYR), first studied by Nimlos et al. with resonant two-photon ionization (R2PI) spectroscopy.[5] In a *cis* amide, both the N−H and C═O hydrogen bonding sites lie on the same side of the molecule and have the potential to anchor a hydrogen-bonded solvent bridge. Held and Pratt later confirmed the bridged 2-PYR−A_1 and 2-PYR−A_2 structures from rotationally resolved fluorescence excitation spectroscopy.[6] Although the separation between the ammonia hydrogen and the carbonyl oxygen in 2-PYR−A_1 was estimated to be quite large for a hydrogen bond, 2.91 Å, the rather high barrier for internal rotation of the ammonia, 424 cm^{-1}, confirmed the presence of the hydrogen bonding interaction.[6]

We have recently obtained R2PI spectra of two additional *cis* amides, oxindole (OI) and 3,4-dihydro-2(1*H*)-quinolinone (DQ), as shown below, and their complexes with one and two ammonia molecules as well as with one to three water molecules.[7] The amide groups in these molecules are less-

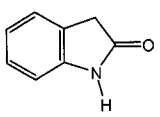

oxindole
(OI)

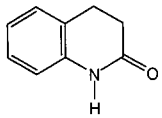

3,4-dihydro-2(1H)-quinolinone
(DQ)

integral parts of the aromatic chromophore than in 2-PYR and hence should provide a better model for the more common aliphatic amides. The observed spectral shifts of the electronic origin transitions of the amide clusters are consistent with

* Corresponding authors.
† E-mail: cable@bgnet.bgsu.edu.
‡ E-mail: zwier@purdue.edu.

10.1021/jp011178q CCC: $20.00
Published on Web 08/10/2001

structures in which a solvent or solvent chain bridges the *cis* amide functional group.

The fundamental hydride stretch region of the IR spectrum should provide a sensitive probe of the structure and hydrogen bonding interactions in these complexes. The results of such a study based on resonant ion-dip infrared (RIDIR) spectroscopy have recently been reported for the water complexes of OI and DQ (OI−W_n, $n = 1-3$, and DQ−W_n, $n = 1, 2$).[8] These confirmed the generality of the bridged binding motif across the *cis* amide group and identified a strong coupling of the hydrogen-bonded XH oscillators within the bridge. The current study presents the results of applying RIDIR spectroscopy to the ammonia complexes of OI and DQ (OI−A_n and DQ−A_n, $n = 1, 2$). As reported herein, the ammonia NH stretch fundamentals in the IR spectra exhibit the characteristic features associated with hydrogen-bonded hydride stretches: shifts to lower frequencies, intensity enhancement, and a degree of spectral broadening. However, relative to hydrogen bond donation by water, the case with ammonia is more complicated due to the presence of three rather than two hydride stretches. This RIDIR study reveals the characteristic spectral signature associated with hydrogen bond donation by ammonia and, using a simple reduced-dimension model, compares the results with analogous water clusters of the same *cis* amides.[8]

The realization that ammonia forms hydrogen-bonded bridges across a *cis* amide group, functioning as both a hydrogen bond donor and a hydrogen bond acceptor, is reminiscent of the more familiar amphoteric solvent, water. This suggests that it should be possible to substitute a single ammonia for either of the bridging waters in the dihydrated complexes of OI and DQ. Both R2PI and RIDIR spectroscopy reveal that such ternary water/ammonia complexes do form, and the IR spectra lead to assignments for two distinct bridge isomers in which either water donates to ammonia or ammonia donates to water. The counterbalancing effects that produce these isomeric structures are discussed herein.

II. Experimental and Theoretical Methods

R2PI and RIDIR spectra were obtained using a previously described molecular-beam time-of-flight mass spectrometer.[9,10] Experimental details were similar to those used to record the spectra of water complexes of the same two amides.[8] Solid ammonium carbonate at room temperature was used to seed the carrier gas with ammonia. The partial pressure of the ammonia above the ammonium carbonate was sufficient to produce ammonia clusters in quantities yielding signal intensities comparable to those of water clusters. Ternary amide clusters could also be formed under these conditions and did not require an additional source of water.

The RIDIR technique enables the IR spectrum of each cluster to be obtained free of interference from other species present in the expansion. In practice, a UV laser is fixed on a vibronic transition of the cluster of interest, creating a steady-state ion signal of a given mass that reflects the ground-state population of the cluster. IR spectra are recorded by preceding the UV pulse with an IR pulse that, when resonant with an IR transition of the monitored species, removes population from its ground state. The absorption is detected as a dip in the ion signal generated by the UV laser pulse that follows. The difference in the R2PI ion signal with and without the IR pulse present is recorded using active baseline subtraction in a gated integrator.

For several clusters, IR−UV hole-burning spectroscopy was used to record separate R2PI spectra of different species appearing in the same mass channel. In this case, a unique IR transition of a given species is chosen on which the IR light source is fixed. The R2PI spectrum is then recorded using active baseline subtraction by tuning the UV laser through the R2PI transitions of interest with the UV laser pulse delayed from the IR laser pulse by about 200 ns.

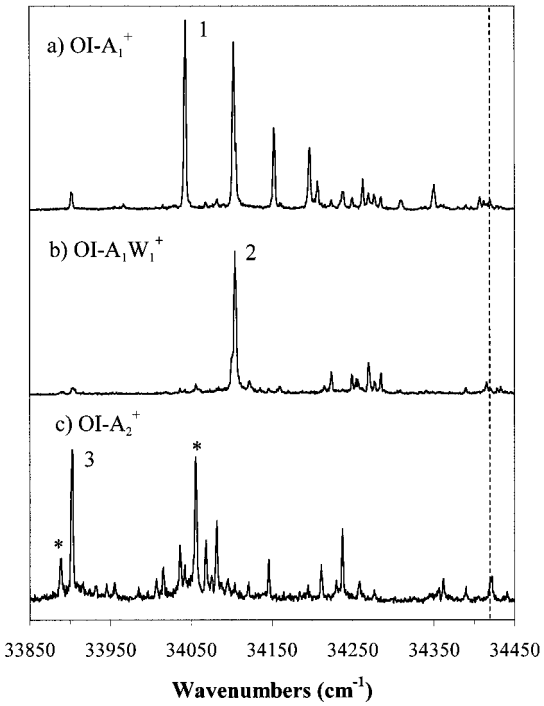

Figure 1. One-color resonant two-photon ionization spectra in the (a) OI−A_1^+, (b) OI−$A_1W_1^+$, and (c) OI−A_2^+ mass channels. The position of the OI monomer origin (34 411 cm^{-1}) is indicated by a vertical dashed line. Numerical labels identify the origin transitions used for RIDIR spectroscopy.

Density functional theory (DFT) calculations employing the Becke3LYP[11,12] functional and a 6-31+G*[13] basis set were used to provide a comparison for the experimental results. Optimized geometries, vibrational frequencies, and IR intensities were computed for the ammonia and ammonia/water complexes of the smaller amide, OI. Binding energies were also calculated but not corrected for basis set superposition error.[14] Only hydrogen-bonded bridge structures were used as starting geometries since Hartree−Fock calculations using a 6-31G** basis set found all other ammonia cluster geometries to lie at considerably higher energies.[7] Harmonic vibrational frequencies were scaled by a factor of 0.976. All calculations were carried out using the Gaussian 98 suite of programs.[15]

III. Results and Analysis

A. R2PI Spectra. R2PI spectra of the OI and DQ clusters are presented in Figures 1 and 2, respectively. All spectra were obtained by monitoring the parent mass of the indicated ion. The origin transitions of all complexes are red-shifted from those of the corresponding free-amide chromophores. The R2PI spectra of the binary ammonia complexes are discussed in more detail elsewhere[7] and are included here to indicate the origin transitions used to monitor the depletion resulting from an IR-induced vibrational transition. With both OI and DQ, the magnitude of the origin red shift is larger for the two-ammonia complexes than for the single-ammonia complexes. The spectrum of OI−A_2 is complicated by an additional weak feature located 12 cm^{-1} to the red of the labeled origin ("3" in Figure 1c). This peak and the strong feature located 155 cm^{-1} to the

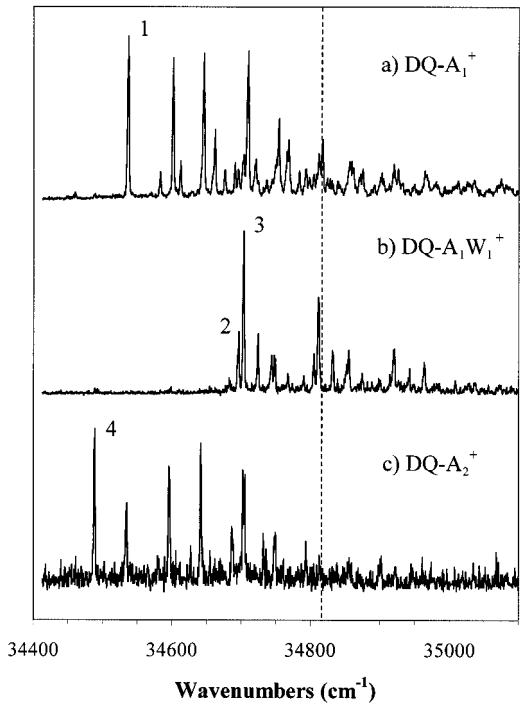

Figure 2. One-color resonant two-photon ionization spectra in the (a) $DQ-A_1^+$, (b) $DQ-A_1W_1^+$, and (c) $DQ-A_2^+$ mass channels. The position of the DQ monomer origin (34 808 cm^{-1}) is indicated by a vertical dashed line. Numerical labels identify the origin transitions used for RIDIR spectroscopy.

blue (both marked by asterisks) appear with intensities relative to the labeled origin that vary with expansion conditions, suggesting their assignment to higher-order clusters. Although this interpretation is confirmed by RIDIR spectroscopy, these larger clusters are not discussed further.

The origin transitions of the ternary water/ammonia clusters are less red-shifted from the monomer origin (Figures 1b and 2b) than the single-ammonia clusters (Figures 1a and 2a). Thus, in $OI-A_1W_1$ a single transition at 34 105 cm^{-1} is assigned to the electronic origin, corresponding to a 306 cm^{-1} red shift, while in $DQ-A_1W_1$ a pair of peaks at 34 697 and 34 704 cm^{-1} with unequal intensities suggests two distinct origins (labeled 2 and 3 in Figure 2), shifted by -111 and -104 cm^{-1} from that of bare DQ, respectively. Only minor vibronic activity is associated with the electronic transition in $OI-A_1W_1$, while the spectrum of $DQ-A_1W_1$ shows substantial activity in a number of low-frequency modes. Progressions based on a 108 cm^{-1} mode can be clearly identified for both origin components. One source of this activity arises from the monomer itself with its puckered six-membered amide-containing ring. A similar progression in a ring-puckering mode is also seen in the R2PI spectrum of bare DQ.[7] The presence of two origin transitions in the spectrum of $DQ-A_1W_1$ would appear to indicate the presence of two distinct cluster structures. This possibility is addressed later in light of results from IR−UV hole-burning spectroscopy, but it should first be noted that close examination of the $OI-A_1W_1$ origin transition reveals a weak shoulder on its low-energy side, which might also be indicative of a second cluster structure.

B. RIDIR Spectra. The RIDIR spectra of the bare amide chromophores have been discussed previously.[8] These show a sharp fundamental NH stretch transition at 3493 (OI) and 3445 cm^{-1} (DQ) and a group of CH stretch fundamentals below 3100 cm^{-1}. The NH stretch fundamentals of the ammonia monomer have been studied at very high spectral resolution and are known to produce a symmetric stretch at 3336 cm^{-1} and a degenerate "antisymmetric" stretch at 3444 cm^{-1}.[16] Upon complexation, and loss of C_{3v} symmetry, the degeneracy of the antisymmetric stretch is broken, thereby producing three distinct ammonia NH stretch fundamentals for each ammonia molecule in the cluster. In the following sections, qualitative assignments of the observed RIDIR spectra are made to orient the reader to the distinguishing features of the spectra. These assignments are considered in more detail in section D following the presentation of the density functional theory calculations in section C.

1. Single-Ammonia Complexes. The RIDIR spectra of $OI-A_1$ and $DQ-A_1$ are shown in Figures 3a and 3b, respectively. Below 3100 cm^{-1}, a series of sharp CH stretch fundamentals is seen at essentially the same frequencies as those observed in the amide monomers. Above 3300 cm^{-1}, the spectra of both $OI-A_1$ and $DQ-A_1$ exhibit three sharp peaks: two intense peaks at 3313 and 3406 cm^{-1} and a relatively weak peak at 3436 cm^{-1}. These are assigned to ammonia NH stretch fundamentals. The 3313 cm^{-1} transition is found 20 cm^{-1} below the symmetric stretch frequency of the ammonia monomer, while the two higher-frequency stretches are 10 and 38 cm^{-1} below the frequency of the degenerate ammonia NH stretch.

The amide NH stretch is expected to shift down in frequency from its value in the bare chromophore if it is involved in hydrogen bond donation to ammonia. In the analogous bridged water clusters, the amide NH stretch fundamental was heavily mixed with the hydrogen-bonded water OH stretch(es), occurring at frequencies of 3376 cm^{-1} in $OI-W_1$ and 3332 cm^{-1} in $DQ-W_1$.[8] Since ammonia is expected to be a stronger hydrogen bond acceptor than water, the amide NH stretches in the ammonia clusters are anticipated at even lower frequencies. Thus, the broad peaks centered near 3230 cm^{-1} in $OI-A_1$ and 3185 cm^{-1} in $DQ-A_1$ are assigned to the amide stretch. These correspond, in both cases, to 260 cm^{-1} shifts from their values in the bare amides.

The amide NH stretch region of the spectrum is complicated by broadening and the appearance of additional substructure. For instance, three underlying peaks at 3214, 3231, and 3250 cm^{-1} can be identified in the broad amide NH stretch fundamental in $OI-A_1$. In $DQ-A_1$, the clump of bands in this region is dominated by a transition at 3184 cm^{-1}, believed to be primarily amide NH stretch in character, but the bands centered at 3142, 3237, and 3248 cm^{-1} also likely gain their oscillator strength from the amide NH stretch through Fermi resonant mixing. The bands at 3237 and 3248 cm^{-1} are close in frequency to the corresponding bands in the $OI-A_1$ spectrum, suggesting that similar Fermi resonances are responsible for the mixing in both OI and DQ.

For comparison with the complexed *cis* amides, ammonia complexes of the closely related *trans* amide *trans-N*-phenylformamide or *trans*-formanilide (TFA) have also been investigated. The RIDIR spectrum of $TFA-A_1$, obtained using the origin transition at 35 673 cm^{-1} to monitor the IR depletion,[17] is displayed in Figure 3c. Because the two hydrogen bonding sites of a *trans* amide lie on opposite sides of the molecule, ammonia functions solely as a hydrogen bond acceptor in this complex. The amide NH stretch in the RIDIR spectrum of $TFA-A_1$ is identified with the intense Fermi resonance doublet at 3275 and 3306 cm^{-1}. In bare TFA, the NH stretch is located at 3465 cm^{-1}, and in the $TFA-W_1$ complex in which water binds at the amide NH site, the NH stretch is found at 3402 cm^{-1}.[18] Thus, the hydrogen bond formed between the amide NH group and ammonia produces a red shift of the NH stretch of approximately 175 cm^{-1}, exceeding that produced upon water

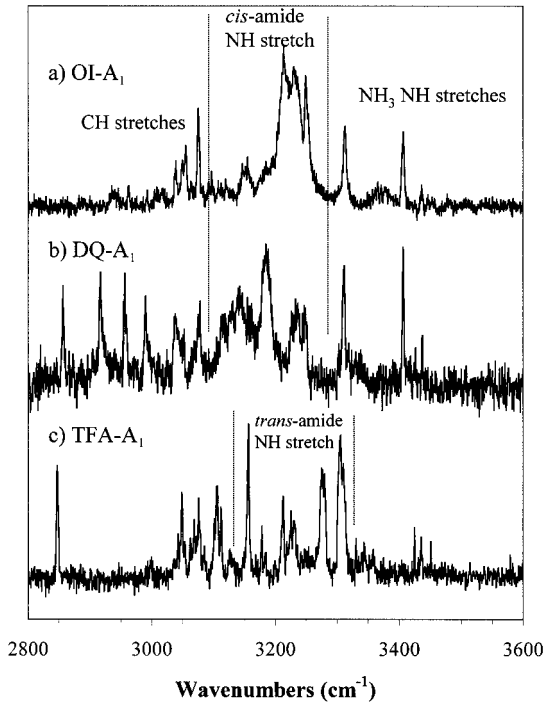

Figure 3. RIDIR spectra of the single-ammonia complexes of the two *cis* amides (a) OI and (b) DQ and of the *trans* amide (c) TFA.

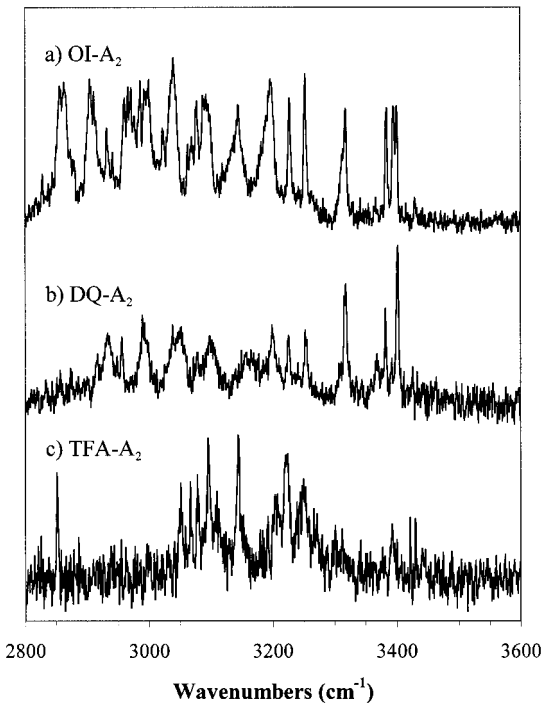

Figure 4. RIDIR spectra of the disolvated ammonia clusters of the two *cis* amides (a) OI and (b) DQ and of the *trans* amide (c) TFA.

complexation by >100 cm^{-1}. From 3150 to 3000 cm^{-1}, a series of aromatic CH stretches is observed, while the aldehyde CH stretch is identified at 2847 cm^{-1}. The location of all CH stretch fundamentals closely parallels that which is seen both in the bare molecule and in the singly hydrated cluster.[8] Two sets of weak, closely spaced peaks starting at 3425 and 3331 cm^{-1} are associated with the antisymmetric and symmetric ammonia NH stretches, respectively, appearing close to those of the free ammonia molecule. Finally, between 3150 and 3250 cm^{-1}, a number of peaks are found that have no counterpart in the spectrum of either the bare molecule or the single-water cluster.[8] These must also be transitions that gain intensity by Fermi resonant mixing with the amide NH stretch. The difference in ammonia's hydrogen bonding environment when complexed to a *cis* or *trans* amide group is clearly evident from the very different pattern of IR absorptions associated with the ammonia NH stretches, consistent with the developing picture that ammonia must be functioning both as a hydrogen bond donor and as a hydrogen bond acceptor in the *cis* amide complexes.

2. Complexes with Two Ammonia Molecules. RIDIR spectra of OI$-A_2$ and DQ$-A_2$ are presented in Figures 4a and 4b, respectively. The most striking and remarkable feature of these spectra is the dense and seemingly irregular pattern of transitions, containing both sharp and broad features, extending from 2800 to 3300 cm^{-1}. Some of the sharp features appear to correlate with fundamental CH stretches seen in the amide monomers,[8] but the broad peaks have no monomer counterparts. The number of bands observed far exceeds the number of NH oscillators, suggesting that the Fermi resonant mixing that began to appear in the single-ammonia complexes (section B.1) is now rampant in the complexes with two ammonia molecules. In this spectral region, the main source of IR transition intensity is expected to be the amide NH stretch (as shown in sections C and D). Further discussion of this Fermi resonance mixing will be delayed until the calculations have been considered.

Fortunately, the extensive Fermi resonance structure has little overlap with the ammonia NH stretch region (>3200 cm^{-1}), which is the primary focus of the present study. If the OI$-A_2$ and DQ$-A_2$ complexes share the same ammonia bridge structure, one might anticipate similar-looking spectra in the ammonia NH stretch region. This is indeed the case since the two RIDIR spectra are nearly identical in the region above 3190 cm^{-1} (Figure 4a,b). In OI$-A_2$, seven transitions are identified at 3196, 3227, 3253, 3319, 3385, 3395, and 3401 cm^{-1}. Each of these has an exact counterpart in the DQ$-A_2$ spectrum if it is assumed that the 3395/3401 cm^{-1} doublet in Figure 4a is a level split by Fermi resonance in OI$-A_2$, which merges to a single peak at 3401 cm^{-1} in DQ$-A_2$ (Figure 4b).

One anticipates a set of six NH stretch fundamentals from the two ammonia molecules in these complexes. Two of these fundamentals may be quite weak free-NH stretches that are expected to appear around 3440 cm^{-1}, but may be hard to observe. The presence of six or seven bands in the region below 3400 cm^{-1} (rather than four) suggests some degree of Fermi resonant mixing even in the ammonia NH stretch region. More specific assignments can only be made following guidance from the calculations of IR frequencies and intensities (section C).

Again for comparison, the RIDIR spectrum of TFA$-A_2$, which cannot adopt a bridged structure, is shown in Figure 4c. This spectrum was obtained by monitoring the 35 565 cm^{-1} origin transition in the mass-resolved R2PI spectrum.[17] The broad IR transition at 3222 cm^{-1} is attributed to the amide NH stretch fundamental, corresponding to a red shift of at least 50 cm^{-1} from its location in TFA$-A_1$. The weak transitions near 3400 and 3440 cm^{-1} are associated with the ammonia stretches and again appear to be quite different than their counterparts in OI$-A_2$ and DQ$-A_2$. Another obvious difference between the TFA$-A_2$ and the *cis*-amide$-A_2$ spectra is the absence of the intense, complex pattern of broad peaks between 2800 and 3200 cm^{-1} in the TFA$-A_2$ spectrum. Instead, all transitions below 3150 cm^{-1} can be assigned to CH stretch fundamentals by comparison to the RIDIR spectrum of bare TFA.[8]

Already at a qualitative level, the striking differences between the spectra of the *cis* and *trans* amide complexes with two ammonia molecules reflect the dissimilar binding environments

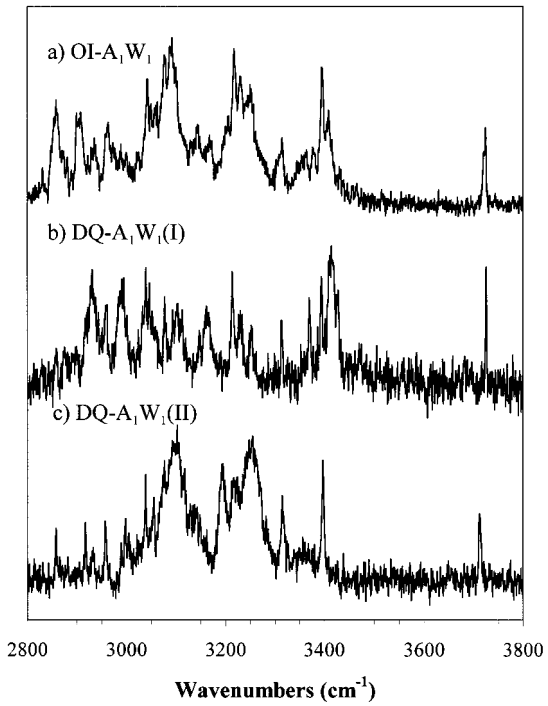

Figure 5. RIDIR spectra of the ternary ammonia/water clusters (a) OI−A_1W_1, (b) DQ−A_1W_1(I), and (c) DQ−A_1W_1(II). Spectra b and c were recorded by monitoring the origin transitions at 34 697 and 34 704 cm^{-1} (labeled 2 and 3 in Figure 2), respectively.

anticipated for the ammonia molecules in the two contexts. At the same time, the similarities in the spectra of the *cis* amide complexes are consistent with a common hydrogen bonding topology. In particular, the shifts to lower frequency and the intensity enhancements of the ammonia NH stretches in the *cis* amide complexes are consistent with a bridged structure in which each ammonia functions as both a hydrogen bond donor and a hydrogen bond acceptor.

3. Ternary Ammonia/Water Clusters. RIDIR spectra of the ternary *cis*-amide−A_1W_1 clusters are shown in Figure 5. The spectrum of OI−A_1W_1 in Figure 5a was obtained by monitoring the single origin in the R2PI spectrum at 34105 cm^{-1}. The spectra in Figures 5b and 5c were obtained by monitoring transitions 2 and 3, respectively, in the R2PI spectrum in the DQ−$A_1W_1^+$ mass channel (Figure 2b). The two DQ−A_1W_1 RIDIR spectra are quite distinct and therefore confirm the presence of two cluster isomers in the supersonic jet expansion. The isomer with the lower frequency origin, denoted as DQ−A_1W_1(I), exhibits a RIDIR spectrum with a water free-OH stretch at 3725 cm^{-1}, an intense and broad transition at 3414 cm^{-1} that most likely corresponds to a hydrogen-bonded OH stretch, three sharp transitions at 3312, 3369, and 3394 cm^{-1}, and a complex pattern of broad peaks below 3200 cm^{-1}. The second cluster isomer, denoted as DQ−A_1W_1(II), has a very different RIDIR spectrum with a free-OH stretch at 3711 cm^{-1}, two sharp transitions at 3315 and 3397 cm^{-1}, and two very broad and intense transitions centered at 3100 and 3250 cm^{-1}. The complex pattern of broad peaks seen below 3200 cm^{-1} in the spectrum of isomer I is absent from the spectrum of isomer II. Instead, several sharp transitions are seen in this region that can be readily assigned to fundamental CH stretches of DQ.

A plausible explanation for the appearance of two cluster isomers of the *cis*-amide−A_1W_1 complexes is the consideration of isomeric bridged structures where the order of the two solvents in the hydrogen-bonded bridge differs: NH···A···W···O═C in one and NH···W···A···O═C in the other. The assignment of the hydrogen-bonded OH stretch in DQ−A_1W_1(I) to the intense transition at 3414 cm^{-1} is done by analogy to the assignment of the hydrogen-bonded OH stretch in the bridged water cluster DQ−W_1, which occurs at 3421 cm^{-1}. In DQ−W_1, the water functions as a hydrogen bond donor to the carbonyl oxygen. The similarity of this transition in DQ−A_1W_1(I) supports its assignment to a bridged structure in which water binds at the carbonyl oxygen and ammonia binds at the amide NH. The appearance of the complex pattern of broad peaks below 3200 cm^{-1} thus appears to be the characteristic signature of an ammonia-bound amide NH stretch in which the ammonia is also part of a hydrogen-bonded bridge. In fact, close inspection of the pattern of transitions in the 2800−3200 cm^{-1} region of the spectra of both DQ−A_1W_1(I) (Figure 5b) and DQ−A_2 (Figure 4b) reveals that the Fermi resonance structure occurs at nearly identical frequencies in the two complexes.

The other bridged structure, DQ−A_1W_1(II), must have an amide NH···W···A···O═C bridge in which the water molecule is bound at the amide NH and also serves as a hydrogen bond donor to ammonia. The two strong bands centered at 3100 and 3250 cm^{-1} in Figure 5c are then amide NH···OH_2 and water OH···NH_3 fundamentals. This spectrum does not suffer from the same severe congestion in the 2800−3200 cm^{-1} region, which has been ascribed to Fermi resonant mixing involving the amide NH stretch. When the *cis* amide NH is hydrogen bonded to water instead of ammonia, even when the water is part of a hydrogen-bonded bridge, the extent of this mixing appears to be reduced.

The RIDIR spectrum of OI−A_1W_1 (Figure 5a**)** was obtained by monitoring transition 2 in Figure 1b. This transition was suspected to be an unresolved doublet analogous to transitions 2 and 3 of DQ−A_1W_1 in Figure 2b, which we have just considered. Consistent with this possibility, the RIDIR spectrum of this transition appears to be a composite spectrum containing the strong absorption features of both DQ−A_1W_1(I) and DQ−A_1W_1(II). Thus, a free-OH stretch appears as a slightly broadened transition at 3723 cm^{-1}; a moderately broad peak at 3409 cm^{-1} correlates with the hydrogen-bonded OH stretch seen at 3414 cm^{-1} in DQ−A_1W_1(I), and the sharp peak which it overlaps at 3395 cm^{-1} has its counterpart in the 3394 and 3397 cm^{-1} transitions in DQ−A_1W_1(I) and DQ−A_1W_1(II), respectively. At lower frequencies, two very broad peaks near 3092 and 3230 cm^{-1}, as in DQ−A_1W_1(II), are seen in the midst of a complex series of broad peaks, reminiscent of DQ−A_1W_1(I). Thus, the origin of the OI−A_1W_1 R2PI spectrum does in fact contain two unresolved transitions associated with the same bridged cluster isomers as those in DQ−A_1W_1.

C. IR−UV Hole-Burning Spectra. Given the unique IR spectra of the two DQ−A_1W_1 structural isomers, UV spectra of each isomer can be recorded free of interference from the other isomer using IR−UV hole-burning methods. To accomplish this, the IR parametric converter was first fixed on the free-OH stretch IR transition of DQ−A_1W_1(I) at 3725 cm^{-1} (Figure 6b) and then on that of DQ−A_1W_1(II) at 3711 cm^{-1} (Figure 6c). The resulting spectra are compared to the R2PI spectrum in Figure 6a. Hole burning clearly reveals that the two origin transitions at 34 697 and 34 704 cm^{-1} arise from two distinct species and further partitions the composite spectrum in Figure 6a into its separate components. Associated with the electronic origin transition of each isomer is a progression in a vibrational mode having a fundamental frequency of 108 cm^{-1}. This correlates well with the 107 cm^{-1} progression-forming vibration in bare DQ associated with a puckering motion of the six-membered amide-containing ring. Several

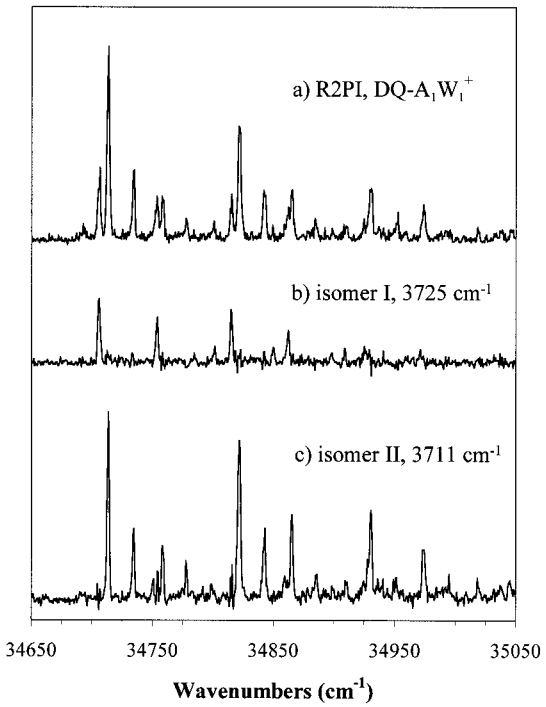

Figure 6. (a) One-color mass-resolved R2PI spectrum of DQ−A_1W_1. (b) R2PI spectrum obtained with the UV pulse following an IR laser pulse fixed at a frequency of 3725 cm^{-1}. (c) R2PI spectrum obtained with the UV pulse following an IR laser pulse fixed at a frequency of 3711 cm^{-1}.

additional low-frequency modes are also evident that must be associated with intermolecular vibrations in the clusters.

D. Density Functional Theory Calculations. To confirm and strengthen the initial structural deductions based on the RIDIR spectra, DFT Becke3LYP/6-31+G* calculations were performed to determine energy-minimized structures, vibrational frequencies, and IR transition intensities for the clusters. These calculations were performed only on complexes containing the OI amide chromophore, and the structures probed were those suggested by the RIDIR spectroscopy.

1. Structures. Table 1 gives an overview of the key structural parameters calculated for the OI−A_n and OI−A_1W_1 complexes at the present level of theory. As anticipated, the optimized structure of OI−A_1 shows evidence of two hydrogen bonds between ammonia and the *cis* amide group. The amide NH−ammonia hydrogen bond is characterized by a heavy atom separation of 2.92 Å and a hydrogen−nitrogen separation of 2.00 Å, while the ammonia NH−carbonyl oxygen hydrogen bond has a slightly shorter heavy atom separation of 2.77 Å but a substantially longer hydrogen−oxygen separation of 2.33 Å. Both hydrogen bond angles deviate significantly from 180°, with that of the amide NH−ammonia being 147° and that of the ammonia−carbonyl oxygen being 136°.

The calculated structure of bridged OI−A_2 shows evidence of three hydrogen bonds. Hydrogen−heavy atom separations of 1.90, 2.06, and 2.06 Å are calculated for the amide NH−ammonia, ammonia−ammonia, and ammonia−carbonyl oxygen hydrogen bonds, respectively. These distances are both shorter and more uniform than those found in OI−A_1 and thus appear to reflect a strengthening of all the hydrogen bonds in the bridge. Of particular note is the fact that the ammonia−ammonia hydrogen bond is characterized by an even shorter hydrogen−nitrogen separation than the amide NH−ammonia hydrogen bond in OI−A_1. Clearly, part of the enhancement of the hydrogen bonding interactions in OI−A_2 is geometrical in nature as a "two-solvent" bridge is of sufficient length and flexibility to effectively span the "jaws" of the *cis* amide group. In fact, in OI−A_2, none of the hydrogen bond angles are found to

TABLE 1: Summary of the Calculated Bond Distances, Heavy Atom Separations, Bond Angles, and Binding Energies for OI, OI−A_{1-2}, and OI−A_1W_1

species	distance[a] (Å)		angle[a] (deg)		binding energy[b] (kcal/mol)	
OI	NH	1.012	OCN	125.6		
	CO	1.219	CNH	121.8		
	NC	1.386				
	(N)H−O(C)	2.631				
OI−A_1	NH	1.029	OCN	125.6	9.3	7.4
	A HB NH	1.024	CNH	120.3		
	A free NH	1.019	NHNA	147.4		
	CO	1.227	NHAO(C)	136.2		
	NC	1.376				
	N(H)−N_A	2.918				
	$N(H)_A$−O(C)	2.772				
	(N)H−N_A	1.999				
	$(N)H_A$−O(C)	2.334				
	(N)H−O(C)	2.611				
OI−A_2	NH	1.040	OCN	126.3	18.3	14.2
	A1 HB NH	1.033	CNH	123.5		
	A1 free NH	1.019	NHNA1	176.5		
	A2 HB NH	1.026	NA1HNA2	162.1		
	A2 free NH	1.019	NHA2O(C)	168.3		
	CO	1.230				
	NC	1.372				
	N(H)−N_{A1}	2.939				
	$N(H)_{A1}$−$N(H)_{A2}$	3.065				
	$N(H)_{A2}$−O(C)	3.070				
	(N)H−N_{A1}	1.901				
	$(N)H_{A1}$−N_{A2}	2.065				
	$(N)H_{A2}$−O(C)	2.059				
	(N)H−O(C)	2.676				
OI−A_1W_1(I)	NH	1.041	OCN	126.5	21.5	17.2
	A1 HB NH	1.026	CNH	123.7		
	A1 free NH	1.019	NHNA1	176.3		
	W2 HB OH	0.986	NHA1OW2	154.0		
	W2 free OH	0.967	OHW2O(C)	172.5		
	CO	1.233				
	NC	1.367				
	N(H)−N_{A1}	2.935				
	$N(H)_{A1}$−O_{W2}	2.943				
	$O(H)_{W2}$−O(C)	2.783				
	(N)H−N_{A1}	1.896				
	$(N)H_{A1}$−O_{W2}	1.986				
	$(O)H_{W2}$−O(C)	1.803				
	(N)H−O(C)	2.681				
OI−A_1W_1(II)	NH	1.031	OCN	126.2	22.2	17.5
	W1 HB OH	1.003	CNH	123.2		
	W1 free OH	0.968	NHOW1	174.6		
	A2 HB NH	1.027	OHW1NA2	164.9		
	A2 free NH	1.019	NHA2O(C)	163.9		
	CO	1.231				
	NC	1.371				
	N(H)−O_{W1}	2.869				
	$O(H)_{W1}$−N_{A2}	2.772				
	$N(H)_{A2}$−O(C)	3.028				
	(N)H−O_{W1}	1.841				
	$(O)H_{W1}$−N_{A2}	1.791				
	$(N)H_{A2}$−O(C)	2.028				
	(N)H−O(C)	2.666				

[a] Atoms in parentheses are used to guide the reader in the specific atom designations and are not used as part of the calculated angles or distances. A1 and A2 and W1 and W2 refer to the bridging ammonia and water molecules, respectively, where the number indicates the position in the bridge ordered from the N−H to the C═O group of OI. [b] Binding energies are given first without and then with zero-point vibrational-energy correction.

TABLE 2: Calculated Harmonic Vibrational Frequencies, Intensities, and Mode Descriptions for Ammonia, OI−A_{1-2}, and OI−A_1W_1 in the IR Hydride Stretch Region

species	frequency[a] (cm^{-1})	intensity[b] (km/mol)	frequency shift (cm^{-1}) NH[c]	W[d]	A[e]	description[f]
ammonia	3376	2			0	A SS
	3508	3			0	A AS
	3508	3			0	A AS
OI−A_1	3251	712	−295			OI NH
	3345	61			−31	A HB(SS)
	3469	29			−39	A HB(AS)
	3502	7			−6	A free
OI−A_2	3053	1297	−494			OI NH
	3217	314			−160	A1 HB(SS)
	3325	246			−52	A2 HB(SS)
	3429	37			−79	A1 HB(AS)
	3454	111			−54	A2 HB(AS)
	3493	4			−15	A1 free
	3495	4			−13	A2 free
OI−A_1W_1(I)	3041	1233	−506			OI NH
	3323	115			−54	A1 HB(SS)
	3394	1040		−304		W2 HB
	3454	98			−54	A1 HB(AS)
	3499	6			−9	A1 free
	3736	109		37		W2 free
OI−A_1W_1(II)	3067	1058		−631		W1 HB
	3228	786	−319			OI NH
	3313	355			−63	A2 HB(SS)
	3454	109			−54	A2 HB(AS)
	3504	8			−4	A2 free
	3713	47		14		W1 free

[a] Calculated frequencies are scaled by a factor of 0.976. [b] Gaussian 98 IR intensities from frequency calculation outputs. [c] Frequency shifts relative to the calculated free-NH stretch of OI (3547 cm^{-1}), scaled by a factor of 0.976. [d] Frequency shifts relative to the calculated average of the symmetric and antisymmetric stretches of water (3698 cm^{-1}), scaled by a factor of 0.976. [e] Frequency shifts relative to the corresponding calculated ammonia NH stretch, scaled by a factor of 0.976. [f] OI NH = hydrogen-bonded NH stretch of OI; A = ammonia and W = water with numbers specifying the position in the hydrogen-bonded bridge ordered from the N−H to the C=O group of OI; HB(AS) = hydrogen-bonded stretch derived from the ammonia antisymmetric stretch; HB(SS) = hydrogen-bonded stretch derived from the ammonia symmetric stretch; free = antisymmetric stretch involving non-hydrogen-bonded ammonia hydrogens. Detailed depictions of the normal modes are given in Figures 8 and 10.

deviate >18° from linearity, with the ammonia−ammonia hydrogen bond showing the largest deviation.

Two bridged structures were optimized for OI−A_1W_1 corresponding to the two different orderings of the ammonia and water molecules in the bridge. Both structures contain three hydrogen bonds, and the structure in which water accepts a hydrogen bond from the amide NH and donates one to ammonia is found to be slightly more stable than the structure in which ammonia accepts the amide NH hydrogen bond and donates one to water by 0.3 kcal/mol with (0.7 kcal/mol without) a zero-point energy correction. In the slightly less stable isomer I, the hydrogen−heavy atom separations are (starting from the amide NH end of the bridge) 1.90, 1.99, and 1.80 Å, while in isomer II, separations of 1.84, 1.79, and 2.03 Å are found. In both isomers, the longest hydrogen bond is that in which ammonia serves as the donor, and the shortest is that in which water serves as the donor. Again, with two solvents in the bridge, there appear to be sufficient length and flexibility to accommodate nearly linear hydrogen bonds. Except for one case, all hydrogen bond angles are found to be within 16° of linearity. The exception arises for the weak ammonia−water hydrogen bond in isomer I, for which a bond angle of 154° is predicted.

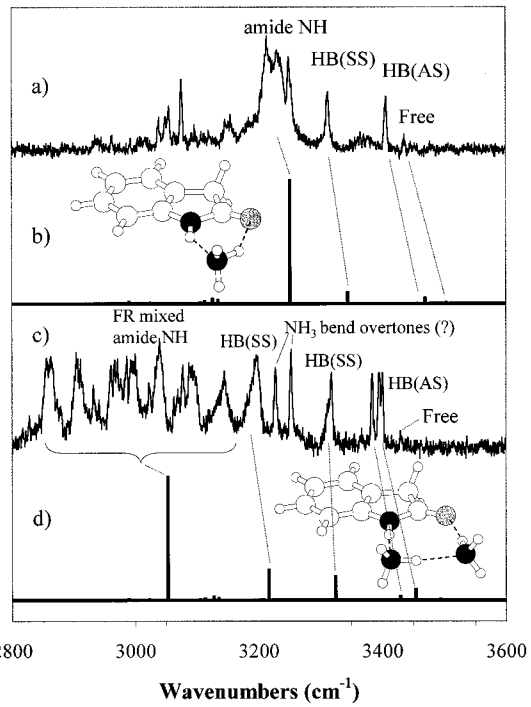

Figure 7. Comparison of the experimental RIDIR spectra of (a) OI−A_1 and (c) OI−A_2 with their respective scaled (factor = 0.976) harmonic vibrational frequencies and intensities (b and d) calculated by DFT with a 6-31+G* basis set.

2. Vibrational Frequencies and IR Intensities. Table 2 displays the calculated harmonic vibrational frequencies scaled by a factor of 0.976, IR transition intensities, and normal mode descriptions of the hydride stretches of OI−A_1, OI−A_2, and the two OI−A_1W_1 structures. These serve as the basis for the comparison with experimental observations, to which we now return.

E. Comparison between Experiment and Theory. *1. Single-Ammonia Complexes.* A visual comparison between the experimental and calculated IR spectra of the OI−A_1 complex is displayed in Figure 7a,b. DFT harmonic frequencies provide a firm basis for assignments of the three ammonia NH stretches in the OI−A_1 cluster. As expected, the degenerate ammonia NH stretch fundamental is split by the asymmetric binding of the ammonia molecule to OI in the complex, resulting in a moderately intense transition at 3469 cm^{-1} and a weak transition at 3502 cm^{-1}. This finding agrees with the earlier assignments of the experimental transitions at 3406 and 3436 cm^{-1} in Figure 7a, connected to the calculated transitions by dashed lines. The third ammonia hydride stretch is predicted to occur with moderate intensity at 3345 cm^{-1}, in close agreement with the observed value of 3313 cm^{-1}. Illustrations of the normal mode motions associated with these vibrations are shown in Figure 8a. The lowest-frequency mode involves an in-phase stretching of all three NH bonds and hence clearly arises from the symmetric stretch of free ammonia despite the presence of the hydrogen bond involving one of the ammonia NH bonds. The mode at an intermediate frequency also involves stretching of all three NH bonds, but here the motion of the hydrogen-bonded hydrogen is out-of-phase with the other two hydrogens. Hence, this mode correlates with one of the degenerate antisymmetric stretches in free ammonia. In what follows, these normal modes are labeled HB(SS) and HB(AS) since both involve substantial motion of the hydrogen-bonded NH. Note that both these transitions lower their frequency and gain considerable IR

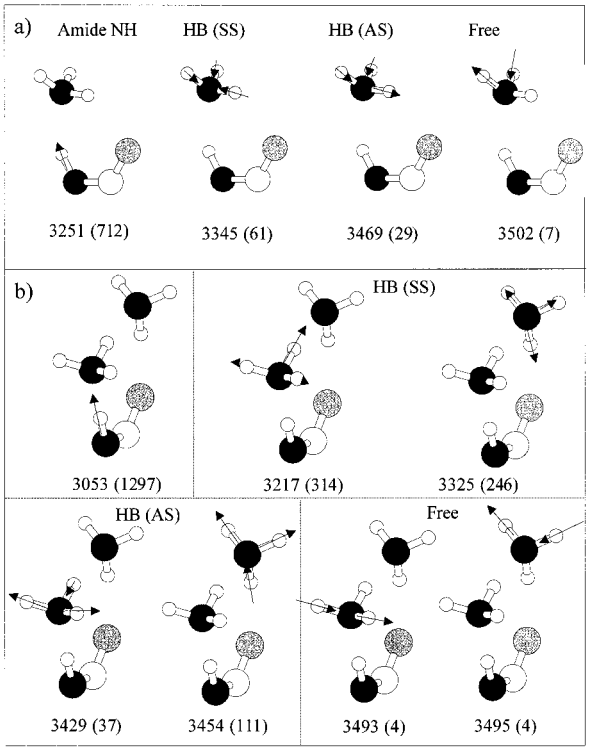

Figure 8. Pictorial representation of the calculated NH stretching normal modes of (a) OI−A_1 and (b) OI−A_2. The direction and magnitude of each contributing motion are indicated by an arrow. For clarity, only the amide group of OI is shown. Scaled frequencies (cm^{-1}) and IR intensities (km/mol, in parentheses) appear below each figure.

intensity when ammonia acts as a hydrogen bond donor, as is typically the case for hydrogen-bonded hydride stretch fundamentals.[19]

The highest-frequency ammonia NH stretch mode in OI−A_1 and DQ−A_1 involves the out-of-phase motion exclusively of the two free hydrogens (Figure 8a), taking on exactly the same form as that of the other member of the degenerate pair of NH stretches in free ammonia. We classify this as the free-NH stretch. Note that in water, the free-OH stretch refers to a single OH bond, while in OI−A_n, the free-ammonia NH stretch is an antisymmetric motion of the two free hydrogens.

The amide NH stretch in OI−A_1 is calculated to have a frequency of 3251 cm^{-1} (Figure 7b), in good agreement with the broad experimental peak centered at 3230 cm^{-1} (Figure 7a). The intensity of this transition is calculated to be >1 order of magnitude larger than the most intense ammonia stretch fundamental. As already noted in section B.1, the broadened experimental amide NH stretch transition also contains distinct substructure arising from Fermi resonances with other vibrational modes. The most likely candidates for the Fermi mixing are overtones of the ammonia NH bends. In free ammonia, the ν_4 bending vibration is degenerate (e symmetry in C_{3v}) and observed at 1626 cm^{-1}. The $2\nu_4$ overtone has both a_1 and e components that appear at 3216 and 3240 cm^{-1}, respectively, and possess a combined transition intensity roughly one-eighth of that of the symmetric NH stretch, $\nu_1(a_1)$, and one-fourth of that of the degenerate NH stretch, ν_3(e).[20] Upon complexation to a near-planar amide group, the degenerate ammonia bend splits into components that are symmetric and antisymmetric with respect to the local symmetry plane. The two bend overtones are symmetric as are the amide NH stretch and in-plane NH bend, while the combination of the two bends is antisymmetric. These ammonia bend overtone levels should be in the right frequency range and of the right symmetry for near-resonant Fermi mixing with the amide NH stretch. Although the magnitude of such mixing might be anticipated to be quite small, animation of the lower-frequency symmetric ammonia bend in OI−A_1 shows that the normal mode also contains a small component of the in-plane amide NH bend that could mediate coupling with the NH stretch. In DQ−A_1 (Figure 3b), the amide NH stretch moves to a lower frequency at 3185 cm^{-1}, but a weaker doublet of peaks remains at 3237 and 3248 cm^{-1}, which may also be associated with ammonia bend overtones.

DFT calculations on TFA−A_1 (not shown) predict a much smaller (3 cm^{-1}) splitting of the degenerate free-ammonia NH stretching vibrations in the case where ammonia acts purely as a hydrogen bond acceptor to the *trans* amide NH group. The IR transition intensities are also predicted to be at least 1 order of magnitude smaller than those in OI−A_1. The spacing between the predicted NH stretching frequencies in TFA−A_1 (3373 and 3495/3498 cm^{-1}) is in reasonable agreement with the two weak sets of peaks seen experimentally starting at 3331 and 3425 cm^{-1}. Thus, when ammonia acts solely as a hydrogen bond acceptor, its NH stretch vibrational frequencies and IR intensities are hardly changed from those of the free molecule. The weakness of the transitions in the absence of hydrogen bond donation is consistent with the reported IR spectrum of the phenol−ammonia complex in which the ammonia stretches were too weak to be observed.[21]

Previous work on the benzene−water complex showed that the intensity of the OH stretch vibration of the water molecule in this complex was distributed among a number of combination bands involving large-amplitude motion of the π-hydrogen-bonded water molecule.[22] A similar effect may account for the multiple peaks seen in TFA−A_1 in the regions of the predicted ammonia NH stretches.

Finally, the amide NH stretch in TFA−A_1 is predicted to occur at 3267 cm^{-1}, placing it once again in close proximity to the expected position(s) of the overtones of the ammonia bends. Experimentally, the amide NH stretch transition is split into several peaks, the two most intense of which appear at 3276 and 3305 cm^{-1} (Figure 3c). Thus, a Fermi resonance interaction, similar to that in OI−A_1, between the amide NH stretch and an overtone of an ammonia NH bend appears to be operative in TFA−A_1.

2. Complexes with Two Ammonia Molecules. DFT calculations provide a firm basis for assigning many of the transitions seen in the complex RIDIR spectra of both OI−A_2 and DQ−A_2. In these complexes, the ammonia NH stretching modes are predicted to be localized on a single molecule with NH displacements on the other ammonia of at most 1.5% of that of the largest displacement on the molecule on which the mode is localized. Figure 8b depicts these normal modes. The six NH stretching vibrations appear in pairs, with the lower-frequency member always localized on the ammonia (A1) that accepts the amide NH hydrogen bond and simultaneously donates a hydrogen bond to the second ammonia (A2). This is in agreement with ammonia being a stronger base than the carbonyl oxygen, and suggests that the ammonia−ammonia hydrogen bond is stronger than the ammonia−carbonyl hydrogen bond. The pair of free-NH stretches is calculated to have the highest frequencies (3493 and 3495 cm^{-1}) but very low transition intensities. We tentatively assign the very weak transition in OI−A_2 at 3429 cm^{-1} to a free-NH stretch, as labeled in Figure 7c.

As expected, the two HB(AS) transitions are calculated to be considerably more intense than the free-NH stretches, and to appear at somewhat lower frequency (3429 and 3454 cm^{-1},

Figure 7d). This suggests the assignment of the single peak at 3385 cm^{-1} and the doublet at 3395 and 3401 cm^{-1} in the RIDIR spectrum of OI−A_2 to these modes. The cause of the splitting of the higher-frequency transition is not clear but may involve combination bands of the hydrogen-bonded NH stretches with a large-amplitude intermolecular mode of the ammonia bridge. Note that the DFT calculations predict that the higher-frequency HB(AS) mode, which is localized on A2, should appear with an intensity 3 times greater than that of the corresponding mode on A1. This agrees with the relative integrated intensities of the peaks in the OI−A_2 spectrum. In DQ−A_2, the HB(AS) transition on A2 is not split (Figure 4b**)** and appears with an intensity 2.5 times that of the HB(AS) transition on A1.

The pair of HB(SS) vibrations are calculated to occur at 3217 and 3325 cm^{-1} (Figure 7d). The higher-frequency member, localized on A2, is in good agreement with the band observed at 3313 cm^{-1}, while the lower-frequency member is tentatively assigned to the intense and broadened peak at 3196 cm^{-1}. Two sharp bands are seen experimentally at 3227 and 3253 cm^{-1} in both OI−A_2 and DQ−A_2 in the region between the two ammonia HB(SS) stretches. We noted previously that these transitions have close counterparts in the single-ammonia cluster spectra. These are then similarly assigned to overtones of the ammonia NH bends, which may also be mixed to some degree with the amide NH bend.

Below 3200 cm^{-1}, only weak CH stretch fundamentals and a single strong amide NH stretch are predicted by the DFT calculations. This contrasts sharply with the experimental observation of a complex pattern of sharp and broad peaks spanning the 300 cm^{-1} region between 2850 and 3150 cm^{-1}. Many of the sharp peaks can be identified as CH stretches, essentially unshifted from their location in the spectra of the monomers or the single-ammonia complexes. The remaining broad peaks must then arise from overtones and combinations that gain intensity through Fermi resonance mixing with the very intense amide NH stretch. DFT calculations predict the NH stretch to occur at 3053 cm^{-1} with a transition intensity of 1297 km/mol, which is >4 times that of any of the ammonia stretches. Note that this frequency is 494 cm^{-1} below that predicted for the bare OI amide NH stretch and 198 cm^{-1} below that predicted for OI−A_1. Thus, in this particular complex, the amide NH stretch is shifted to a lower-frequency region, which apparently results in extensive mixing with a large number of nearly resonant overtones and combinations of other vibrational modes. Since other complexes in the data set suffer from a similar explosion of Fermi resonant mixing, any explanation must be common to the entire set of complexes involved. As such, they are discussed as a whole in section 4.

3. Ternary Ammonia/Water Complexes. Harmonic frequency calculations for the two isomers of OI−A_1W_1 predict substantially different IR spectra. Experimentally, the two cluster isomers have overlapping electronic origin transitions, permitting only a composite RIDIR spectrum to be recorded. Fortunately in DQ−A_1W_1, the two electronic origins are sufficiently resolved so that RIDIR spectra can be obtained for each isomer free of interference from the other. A comparison of the experimental data for DQ−A_1W_1 with the IR spectra calculated for the two OI−A_1W_1 isomers is displayed in Figure 9. On the basis of calculations on OI−W_n and DQ−W_n clusters,[8] we anticipated the differences between the calculated spectra of OI−A_1W_1 and DQ−A_1W_1 to be small.

(a) Isomer II. The predicted spectrum for cluster isomer II (Figure 9d), in which the solvent bridge involves hydrogen bond donation from water to ammonia, is seen to be in very good agreement with the experimental spectrum (Figure 9c) obtained by monitoring transition 2 in Figure 2b. Figure 10b depicts the motions associated with each of the hydride stretch modes. It can be seen that, unlike the case for *cis* amide water clusters,[8] each normal mode involves motions largely localized on a single molecule. The free and hydrogen-bonded water OH stretches are predicted to occur at 3713 and 3067 cm^{-1}, respectively, and correspond with the sharp transition seen at 3711 cm^{-1} and the very broad and intense peak at 3100 cm^{-1}. Clearly, the hydrogen bond in which water donates to ammonia in isomer II is quite strong and produces a very large shift in the frequency of the water OH stretch ($\Delta\nu \approx 600$ cm^{-1}). An interesting comparison can be made to the IR spectrum of the water−ammonia complex isolated in an argon matrix, where the free-OH stretch is found at 3702 cm^{-1} and the hydrogen-bonded OH stretch is seen 267 cm^{-1} lower in frequency at 3435 cm^{-1}.[23] Evidently, hydrogen bond donation from water to ammonia is strengthened significantly when the dimer is part of a cooperatively strengthened NH···OH_2···NH_3···O═C bridge.

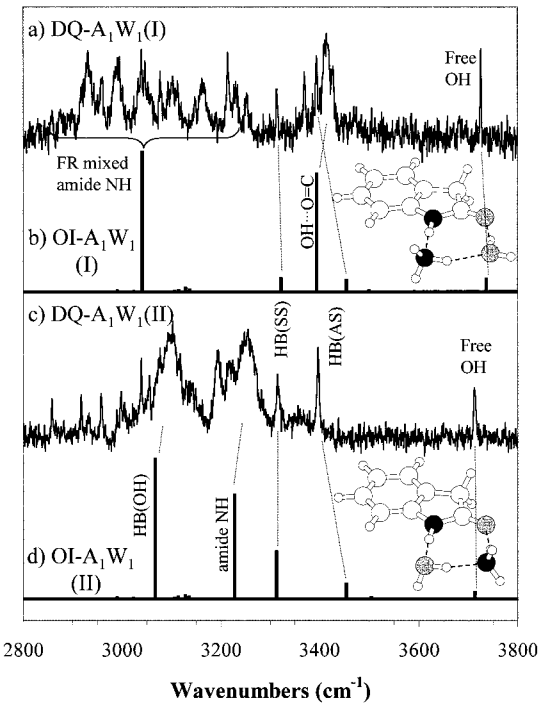

Figure 9. Comparison of the experimental RIDIR spectra of (a) DQ−A_1W_1(I) and (c) DQ−A_1W_1(II) with the scaled (factor = 0.976) harmonic vibrational frequencies and intensities calculated for (b) OI−A_1W_1(I) and (d) OI−A_1W_1(II) by DFT with a 6-31+G* basis set.

As pictured in Figure 9d, the ammonia HB(SS) and HB(AS) fundamentals of isomer II are calculated to occur at 3313 and 3454 cm^{-1}, respectively, matching the two sharp peaks seen in the RIDIR spectrum at 3312 and 3394 cm^{-1}. The free-ammonia NH stretch is predicted to occur at 3504 cm^{-1} with an intensity 13 times less than that of the HB(AS) and cannot be definitively assigned in the experimental spectrum. Finally, an intense transition is predicted to occur for the amide NH stretch at 3228 cm^{-1}, in good agreement with the very broad and intense peak seen at 3250 cm^{-1}. Thus, the amide NH stretch occurs at a higher frequency than the hydrogen-bonded OH stretch in isomer II because of the weaker hydrogen bond formed by the amide NH when water rather than ammonia is the acceptor.

(b) Isomer I. The spectrum predicted for cluster isomer I, in which the solvent bridge involves hydrogen bond donation from ammonia to water (Figure 9b), also matches reasonably well with the experimental DQ−A_1W_1(I) spectrum (Figure 9a) once

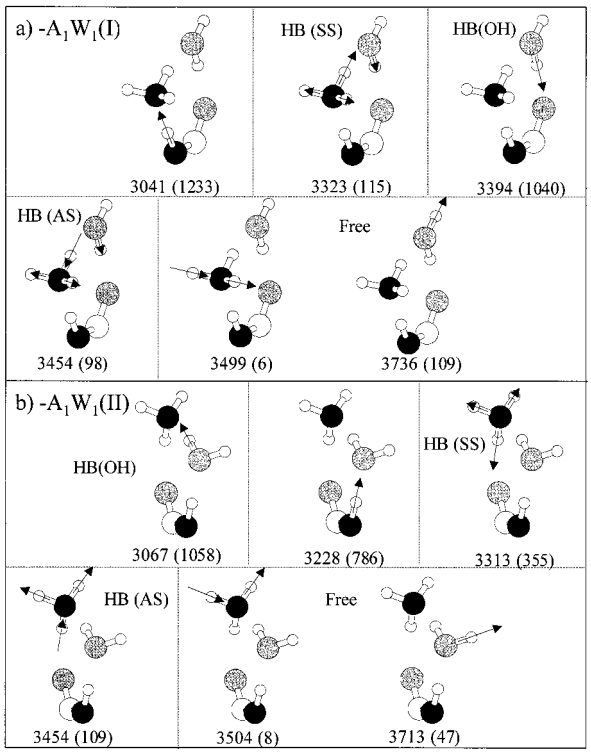

Figure 10. Pictorial representation of the calculated normal modes of the NH and OH stretch vibrations for the two isomers of the ternary ammonia/water clusters (a) OI−A_1W_1(I) and (b) OI−A_1W_1(II). Only the amide group of OI is shown. The direction and magnitude of each contributing motion are indicated by an arrow. Scaled frequencies (cm^{-1}) and IR intensities (km/mol, in parentheses) appear below each figure.

one recognizes that most of the structure below 3200 cm^{-1} in the experimental spectrum is to be assigned to the amide NH stretch. Below 3300 cm^{-1}, the DFT calculations predict only a single intense peak corresponding to the amide NH stretch at 3041 cm^{-1} with an intensity of 1233 km/mol. This frequency is 200 cm^{-1} lower than that in isomer II, while the intensity is 65% greater. Experimentally, the complex pattern of sharp and broad peaks is reminiscent of the Fermi resonant mixing that occurs when two ammonia molecules are in the bridge. As in that case, the NH stretch is very intense and is shifted to a sufficiently low frequency that strong Fermi resonance interactions are turned on; this leads to the fractionation of the amide NH stretch transition strength among a number of overtone and combination modes in a pattern characteristic of the DQ or OI molecule.

Free-OH and hydrogen-bonded OH stretches of the water molecule in the complex are calculated to have frequencies of 3736 and 3394 cm^{-1}, respectively, corresponding closely to the sharp peak observed at 3725 cm^{-1} and the broader peak centered at 3416 cm^{-1}. This hydrogen-bonded OH stretch frequency is noticeably lower than that in other clusters where water hydrogen bonds to a carbonyl oxygen. In tropolone−W_1[24] and TFA−W_1,[18] this fundamental is observed at 3506 and 3513/3536 cm^{-1}, respectively. The shift to a lower frequency in DQ−A_1W_1(I) indicates a cooperative strengthening of the water−carbonyl hydrogen bond due to the incorporation of the water into the ammonia−water hydrogen-bonded bridge.

The ammonia HB(SS) and HB(AS) stretches of isomer I are predicted to occur at 3323 and 3454 cm^{-1}, respectively. The lower frequency of these stretches matches well the sharp transition seen at 3313 cm^{-1}, a frequency identical to that in isomer II. The frequency of the HB(AS) mode appears to be overestimated by the calculation, as it is in isomer II and nearly all the other complexes. Here, this overestimation is magnified because it leads to a swap in the positions of the ammonia HB(AS) and hydrogen-bonded OH stretch fundamentals between experiment and calculation. We tentatively assign the sharp peak at 3394 cm^{-1} to the HB(AS) fundamental, in agreement with its value in isomer II. This leaves the nearby sharp peak of comparable magnitude at 3370 cm^{-1} unassigned.

As noted earlier, the spectra calculated for the two isomers of OI−A_1W_1 were compared with the RIDIR spectra of the two DQ−A_1W_1 isomers because the R2PI transitions associated with these isomers were resolved, while those in OI−A_1W_1 were not. However, with the assignments based on the DQ−A_1W_1 spectra in hand, it is also possible to assign the main features of the OI−A_1W_1 spectrum to a composite of spectra from isomers I and II (Figure 5a). Below 3000 cm^{-1}, evidence of extensive Fermi resonance interaction in the OI−A_1W_1(I) isomer is seen. The broad bands centered at 3092 and 3230 arise from the hydrogen-bonded OH and amide NH stretches, respectively, in the OI−A_1W_1(II) isomer. The moderately broad peak at 3409 cm^{-1} corresponds to the hydrogen-bonded OH stretch in OI−A_1W_1(I). Both isomers appear to have fairly similar ammonia HB(SS) and HB(AS) stretches and water free-OH stretches, leading to slightly broadened peaks at 3315, 3395, and 3723 cm^{-1}, respectively.

IV. Discussion and Conclusions

A. Cluster Structures with Ammonia Serving as a Hydrogen Bond Donor. In most elementary discussions of hydrogen bonding, ammonia serves as a common example of a good hydrogen bond acceptor. Its function as a hydrogen bond donor is typically ignored or dismissed. Unusual circumstances appear to be required before ammonia will take on the function of hydrogen bond donation. The hydrogen-bonded bridges studied in this work, in which the ammonia molecule(s) spans the *cis* amide group, provide just such circumstances. We have seen several examples of ammonia-containing bridges in which ammonia serves as a hydrogen bond donor to the carbonyl group (OI−A_1, DQ−A_1, OI−A_1W_1(II), DQ−A_1W_1(II)), to ammonia (OI−A_2, DQ−A_2), and to water (OI−A_1W_1(I), DQ−A_1W_1(I)). In all cases, it is the close proximity of donor and acceptor *cis* amide hydrogen bonding sites that opens the possibility for bridge formation involving ammonia. Furthermore, by tying up the ammonia lone pair in one hydrogen bond in the bridge, the NH groups of ammonia must take part in hydrogen bond donation if the stabilizing effects of bridge formation are to be realized. The N−H and C═O *cis* amide sites orient and stabilize the two-solvent bridges by providing a hydrogen bonding template that can accommodate and stabilize even relatively weak hydrogen bonds by providing cooperative strengthening and structural integrity.

In the current work, hydrogen bond donation by ammonia has been revealed by RIDIR spectroscopy, where changes in the ammonia hydride stretches are consistent with ammonia acting as a hydrogen bond donor. These IR data complement the structural data on the ammonia-containing complexes of 2-PYR, another *cis* amide, reported by Held and Pratt.[6] In the 2-PYR−A_1 complex, hydrogen bond donation to the carbonyl group leads to a considerable distortion of the more conventional hydrogen bond between the amide NH group and ammonia. Interpretation of the rotational constant data for 2-PYR−A_1 led to an N−H···N bond angle that deviated from linearity by 26°.[6] Similarly, the current DFT calculations on OI−A_1 predict a deviation of 33°. These same calculations also find that the local

C_3 axis of ammonia deviates from a line connecting the ammonia nitrogen with the amide hydrogen by 25°. In addition, in the work of Held and Pratt on 2-PYR−A_1, the presence of a substantial attraction between ammonia and the carbonyl group of the *cis* amide was reflected in the high barrier for the internal rotation of ammonia in the complex.[6]

The calculated structure of OI−A_1 is qualitatively similar to that of 2-PYR−A_1. DFT geometry optimization of OI−A_1 yields an ammonia nitrogen−amide hydrogen separation of 2.00 Å and an ammonia hydrogen−carbonyl oxygen separation of 2.33 Å. The latter value is significantly shorter than that obtained by the model of Held and Pratt for 2-PYR−A_1, 2.91 Å, under the assumption that the geometries of neither 2-PYR nor ammonia were altered upon complexation.[6] However, fully optimized structures of 2-PYR−A_1 have since been reported at the MP2 level by Del Bene[25] and from DFT calculations by Dkhissi et al.[26] These MP2 and DFT studies found much smaller hydrogen−oxygen separations of 2.20 and 2.22 Å, respectively, considerably closer to that calculated for OI−A_1. The calculations also accurately reproduce the hydrogen bond angle, 154°, and heavy atom separation, 2.94 Å, in the amide NH−ammonia hydrogen bond derived from the experimental rotational constants.[6] In comparing hydrogen bond geometries in OI−A_1 and 2-PYR−A_1, one should remember that in OI, the amide is contained in a five-membered ring that effectively leads to an opening of the jaws of the *cis* amide group by about 0.2 Å relative to what is found in the six-membered ring of 2-PYR.[8]

When a second ammonia molecule is added to the bridge, an ammonia−ammonia hydrogen bond is formed in which one of the ammonia molecules acts as a hydrogen bond donor to the other. The strengthening of the hydrogen bonds along the bridge is seen clearly in the calculated value, 3.06 Å, for the separation between the two ammonia nitrogens in OI−A_2. This is nearly 0.2 Å shorter than their separation in the free ammonia dimer.[2] Dkhissi et al. have performed similar DFT calculations on 2-PYR−A_2, yielding a 3.04 Å nitrogen−nitrogen separation.[26] Thus, the presence of the *cis* amide template clearly increases the strength of the ammonia−ammonia interaction. With each molecule in the cyclic structure serving as both a hydrogen bond donor and a hydrogen bond acceptor, cooperative effects appear to be substantial.

The stabilizing effect of the *cis* amide template is even more apparent in the case of the ammonia/water complexes. While both HOH···NH_3 and NH_3···OH_2 bridge structures are found in OI−A_1W_1 and DQ−A_1W_1 clusters, only the HOH···NH_3 structure has been observed in the isolated ammonia−water dimer[27] or in low-temperature matrixes.[23] A heavy atom separation of 2.97 Å was deduced for the isolated HOH···NH_3 cluster from fits to rotational constants.[27] Later MP2/aug-cc-VTZ level optimizations on this cluster yielded an oxygen−nitrogen separation of 2.92 Å.[4] These values exceed that calculated for OI−A_1W_1(II) by nearly 0.2 Å. Consistent with this finding is the much lower frequency (∼3100 cm^{-1}) found for the hydrogen-bonded OH stretch in either OI−A_1W_1(II) or DQ−A_1W_1(II), compared to the frequency of 3435 cm^{-1} for the ammonia−water complex observed in the matrix-isolation FTIR experiment.[23]

The ammonia−water complex in which water serves as a hydrogen bond donor corresponds to a minimum on the intermolecular potential-energy surface at the MP2 level of theory, while a structure with the roles of ammonia and water reversed does not.[4,28] Nevertheless, a complex in which ammonia serves as the hydrogen bond donor has been optimized with enforced C_s symmetry at the MP2/6-311+G(2df,2p) level of theory.[28] This resulted in a structure with a heavy atom separation of 3.24 Å and a binding energy that was 3.82 kcal/mol less than that calculated for the experimentally observed structure. However, in the case of either OI−A_1W_1(I) or DQ−A_1W_1(I), both experiment and theory unequivocally indicate that the bridge structure with ammonia donating a hydrogen bond to water is indeed a local potential minimum. Furthermore, the ammonia−water heavy atom separation in OI−A_1W_1(I) is calculated to be nearly 0.3 Å shorter than that calculated for the free ammonia−water complex.[28]

Although the two OI−A_1W_1 isomers are calculated to have very similar energies, their individual stabilizations arise in different manners. OI−A_1W_1(II) is characterized by a very short and strong water−ammonia hydrogen bond that produces a very large red shift in the frequency of the hydrogen-bonded OH stretch. In contrast, OI−A_1W_1(I) exhibits a much longer and weaker ammonia−water hydrogen bond but a much stronger amide NH−ammonia hydrogen bond. It is this strong interaction that shifts the amide NH stretch down in frequency into a region where extensive Fermi resonance coupling is possible.

B. Hydride Stretches in Hydrogen-Bonded Ammonia. The RIDIR spectra of the *cis*-amide−A_n and *cis*-amide−A_1W_1 complexes show clear evidence that the NH stretch fundamentals of ammonia respond to hydrogen bond donation in much the same way as other hydride stretch fundamentals: they shift to a lower frequency, gain intensity, and broaden. However, unlike the case of water where the formation of a hydrogen bond with one OH group localizes the vibrations into hydrogen-bonded OH and free-OH stretches, in ammonia, two vibrations involve substantial motion of the hydrogen-bonded NH group (Figures 8 and 10). In seeking a deeper understanding of the response of the ammonia NH stretches to hydrogen bond formation, we have carried out a series of reduced-dimension normal mode calculations that includes only the three NH stretch internal coordinates of each ammonia molecule in the cluster. Our goal is to see whether such a simple model can correctly reproduce the frequency shifts and intensity changes observed experimentally and calculated by the full normal mode calculations.

Recall that in the isolated ammonia molecule, the hydride stretch fundamentals appear as a nondegenerate symmetric stretch at 3336 cm^{-1} and a doubly degenerate stretch at 3444 cm^{-1}. In terms of the NH stretching internal coordinates, the three oscillators can be modeled as having three identical stretching force constants (643 N/m), corresponding to uncoupled frequencies of 3408 cm^{-1} and an interbond coupling of −36 cm^{-1}. For comparison, the OH stretches in isolated water, with fundamental frequencies of 3656 and 3756 cm^{-1}, would be modeled as two OH oscillators having unperturbed frequencies of 3706 cm^{-1} and force constants of 767 N/m with an interbond coupling of −50 cm^{-1}.

Hydrogen bond donation by either solvent is modeled as a decrease in the force constant of the oscillator that participates in the hydrogen bond. In the case of ammonia, this breaks the 3-fold symmetry of the problem and lifts the degeneracy of the higher-frequency antisymmetric stretch. As the force constant of the hydrogen-bonded oscillator is progressively lowered, the interbond coupling becomes relatively less important and the symmetric stretch of either molecule ultimately evolves into a localized stretch of the hydrogen-bonded oscillator.

If the force constant of the hydrogen-bonded N−H oscillator in ammonia is lowered by 21.9 N/m (∼3%) but the interbond coupling remains unchanged, the three NH stretch fundamentals are predicted to occur at 3309, 3413, and 3444 cm^{-1}. This reasonably simulates the stretching frequencies observed in OI−

TABLE 3: Summary of the Reduced Dimensionality Calculations for the NH Stretching Normal Modes of Ammonia

species[a]	exp. freq (cm^{-1})	calcd freq[b] (cm^{-1})	eigenvectors[b] HB NH	free NH	free NH	ΔF (N/m)	exp. rel. int.	sim.[c] rel. int.	dipole deriv. factor	description[d]
A	3336	3336	0.577	0.577	0.577	0.0		0.29	1.0	SS
	3444	3444	0.816	−0.408	−0.408			1.0		AS
	3444	3444	0.000	0.707	−0.707			1.0		AS
A in OI−A_1	3313	3309	0.780	0.443	0.443	−21.9	1.2	1.1	5.2	HB(SS)
	3406	3413	0.626	−0.551	−0.551		1.0	1.0		HB(AS)
	3436	3444	0.000	0.707	−0.707		0.15	0.10		free
A1 in OI−A_2	3196	3196	0.961	0.196	0.196	−72.4	3.1	3.1	6.6	HB(SS)
	3385	3387	0.278	−0.679	−0.679		0.57	0.44		HB(AS)
	3430	3444	0.000	0.707	−0.707		0.06	0.11		free
A2 in OI−A_2	3319	3309	0.777	0.445	0.445	−21.5	1.1	1.1	5.1	HB(SS)
	3398	3413	0.629	−0.550	−0.550		1.0	1.0		HB(AS)
	3430	3444	0.000	0.707	−0.707		0.06	0.11		free

[a] A = ammonia with numbers specifying the position in the hydrogen-bonded bridge ordered from the N−H to the C=O group of OI. [b] Calculated with an uncoupled NH stretching frequency of 3408 cm^{-1} and an interbond coupling of −36 cm^{-1} with the force constant of the hydrogen-bonded oscillator reduced by the amount shown. [c] Calculated with the magnitude of the dipole-moment derivative of hydrogen-bonded ammonia NH stretch enhanced by the factor shown in the following column. [d] AS = antisymmetric stretch; SS = symmetric stretch; HB(AS) = hydrogen-bonded stretch derived from the ammonia antisymmetric stretch; HB(SS) = hydrogen-bonded stretch derived from the ammonia symmetric stretch; free = antisymmetric stretch involving non-hydrogen-bonded ammonia hydrogens. Detailed depictions of the normal modes are given in Figures 8 and 10.

A_1. The results of this simulation are presented in Table 3. With this rather small change in one force constant, the forms of the normal modes are not significantly altered from those of free ammonia. In particular, the hydrogen-bonded NH stretch is not localized significantly. Both the 3309 and 3413 cm^{-1} modes contain a contribution from the hydrogen-bonded NH stretch, consistent with both their depictions from DFT calculations as shown in Figure 8 and their labeling as HB(SS) and HB(AS) throughout this work. In comparison, the water hydride stretches in OI−W_1[8] are reasonably reproduced by lowering the force constant of the hydrogen-bonded OH oscillator by 110 N/m (or ∼14%). Under these conditions, the coefficients associated with the individual OH oscillators comprising the OH stretch normal modes have magnitudes of 0.985 and 0.172, indicative of essentially localized free and hydrogen-bonded stretches. The hydrogen-bonded stretch is predicted to be red-shifted 236 cm^{-1} from the symmetric stretch, or 286 cm^{-1} from the uncoupled oscillator frequency, in free water. This is exactly the trend expected since water is inherently a much stronger hydrogen bond donor than ammonia.

A similar analysis can be carried out on the OI−A_2 complex. The full normal mode calculations show that the NH stretch modes are localized on a single ammonia molecule. Therefore, the simulation assumes zero coupling between NH oscillators on different ammonia molecules. As before, we attempted to fit the experimental frequencies simply by lowering the diagonal force constants of the two hydrogen-bonded NH oscillators in the bridge, keeping the off-diagonal coupling terms at their values in free ammonia. Ammonia A1 is involved in a stronger hydrogen bond than ammonia A2 since the former donates to ammonia while the latter donates to the carbonyl group. As shown in Table 3, a reasonable reproduction of the three observed fundamental frequencies in ammonia A1 can be obtained with an 11% reduction of the force constant of the hydrogen-bonded NH oscillator. A smaller 3% reduction is required to reproduce the fundamental frequencies in the second ammonia. The coefficients describing the HB(SS) mode in ammonia A1 under these conditions are 0.961 for the hydrogen-bonded NH oscillator and 0.196 for the other two oscillators. Thus, the vibrational displacement is quite localized on the hydrogen-bonded NH oscillator in a manner that is very similar to what is commonly seen with the OH stretch in hydrogen-bonded water. This is also evident from the depictions of the full normal modes shown in Figure 8b.

These simple reduced-dimension calculations can also provide insight into the intensity enhancement observed in two of the three NH stretch fundamentals that contain a significant component of the hydrogen-bonded oscillator. The experimental RIDIR spectrum of OI−A_1 has integrated intensities for the HB(SS) and HB(AS) modes that are 7.6 and 6.6 times, respectively, that of the free-NH stretch mode that involves no displacement of the hydrogen-bonded hydrogen (Table 3). The dipole moment derivatives associated with each of the NH oscillators in isolated ammonia are equivalent in magnitude. However, upon hydrogen bond formation, the magnitude of the dipole derivative of the hydrogen-bonded oscillator is expected to increase as it does in other hydride stretch fundamentals. The degree to which this particular dipole derivative is enhanced can be estimated from the experimental relative intensities. Using the eigenvectors obtained from the frequency simulations, we can obtain a prediction of the relative intensities. This is done through a simple vectorial addition of the two equivalent dipole moment derivatives of the free-NH oscillators to that of the hydrogen-bonded NH oscillator, which is scaled by an enhancement factor (designated as the dipole derivative factor in Table 3) chosen to best fit the experimental relative intensities.

The dipole derivative factors thus obtained are substantial (5.1−6.6) but are consistent with the intensity enhancements obtained for other hydrogen-bonded XH groups.[19] These enhancement factors correlate well with the anticipated strengths of the hydrogen bonds in which the particular ammonia is involved. For instance, when ammonia donates a hydrogen bond to the carbonyl oxygen, as in OI−A_1 or ammonia A2 in OI−A_2, comparable enhancement factors near 5.1 are obtained. This also is in agreement with the similar values derived for the reductions of the force constants of their hydrogen-bonded oscillators. A larger enhancement factor, 6.6, is obtained for ammonia A1 in OI−A_2, which donates to a much stronger acceptor (ammonia A2), consistent with the larger reduction in the force constant of its hydrogen-bonded oscillator.

In *cis*-amide−A_2 complexes, these enhancement factors correctly predict not only that the intensity of the HB(SS) transition in A1 is larger than that in A2 but also that the relative intensities of the HB(AS) transitions in the two ammonia molecules are reversed. In both the OI−A_2 and DQ−A_2 complexes, the experimental intensity of the transition associated with ammonia A1 is only about half that of ammonia A2 despite the fact that A1 is more strongly hydrogen-bonded than A2 (in

OI−A_2, the HB(AS) fundamental appears as a doublet). Although ammonia A1 experiences a larger enhancement of its dipole derivative, the strong hydrogen bond it forms causes the motion of the hydrogen-bonded oscillator to localize in the HB(SS) mode. As a result, the HB(AS) mode in A1 looks more like a free-NH_2 symmetric stretch and its fundamental transition appears with lower intensity. Thus, in a single complex, we find examples of two ammonia hydrogen bonds with substantially different strengths; these are manifested in quite different hydride stretch frequencies and different relative intensity patterns.

C. Fermi Resonance Mixing of the Amide NH Stretch. One of the most striking aspects of several of the RIDIR spectra of the disolvated *cis* amides presented in this work is the extensive series of bands that appears between 2800 and 3200 cm^{-1} when the amide NH stretch fundamental is shifted into this region. This development was completely unanticipated on the basis of the RIDIR spectra of the OI−W_n and DQ−W_n clusters[8] and also differs significantly from what is seen with the single-ammonia complexes. In the latter case, the amide NH stretch fundamental can be clearly identified around 3200 cm^{-1} with only modest substructure that appears to arise from a weak Fermi resonant interaction with the ammonia bend overtones. However, extensive broadening and fractionation of a fundamental XH stretch transition is a rather common occurrence in the IR spectra of strongly hydrogen-bonded X−H···Y complexes.[19] A quantitative account of the broadening and substructure has been the subject of numerous investigations spread over several decades.[29−37] Two primary mechanisms are commonly accepted as contributors to this breadth and substructure:[33,37] (i) strong, anharmonic coupling between the XH stretch and hydrogen bond stretch vibrations and (ii) Fermi resonance mixing of the XH stretch(es) with overtones of the bending modes.

In a recent investigation of the benzoic acid dimer[38] we have studied the OH stretch region of the IR spectrum using RIDIR spectroscopy under jet-cooled conditions that ensure that the spectrum arises exclusively from the zero-point level of the dimer. The structure of this cyclic hydrogen-bonded dimer bears a number of similarities to those of the *cis* amide clusters studied here. Instead of a single broad OH stretch fundamental, a complex pattern of peaks spanning >500 cm^{-1} was observed. Ab initio methods were used to calculate the magnitude of the cubic anharmonic force constants coupling the OH stretch to the intermolecular stretch and to the OH bend. The latter term was calculated to be unusually large (~370 cm^{-1}) and >10 times greater than the coupling to the intermolecular stretch (~24 cm^{-1}). These model anharmonic terms were then mapped onto the normal modes to simulate the IR spectrum. No "pure" OH bending mode was found to exist. Instead, the OH bend is extensively mixed with several other vibrations of similar frequency. As a result, the large stretch−bend anharmonicity constant spreads the OH stretch oscillator strength over some 10−15 transitions. Furthermore, the pattern of transitions predicted by the calculation qualitatively matched the observed structure.

The RIDIR spectra reported in the present work similarly suggest that it is a large NH stretch−NH bend anharmonic coupling that is responsible for the set of bands observed in the amide NH stretch region. As in the benzoic acid dimer case, inspection of the normal modes calculated for bare OI also shows that no single mode is a pure NH bend. Instead, nine normal modes with frequencies between 1217 and 1630 cm^{-1} are found that contain substantial components of NH bending motion. In general, these appear to be mixed NH/CH bends. Overtones and combinations of these modes would fall in the frequency range in which a 2:1 Fermi resonance interaction with the amide NH stretch would be feasible. In the RIDIR spectrum of OI−A_2 (Figure 4a), seven broad peaks can be identified in this region at 2860, 2905, 2970, 2995, 3040, 3090, and 3145 cm^{-1}. Except for the 2995 cm^{-1} peak, exact counterparts for each can be found in the RIDIR spectrum of OI−A_1W_1 (Figure 5a**)**, although the comparison is complicated by the presence of two cluster isomers. The 1:1 correspondence is also apparent in the RIDIR spectra of DQ−A_2 (Figure 4b**)** and DQ−A_1W_1(I) (Figure 5b), with broad peaks found at 2935, 2990, 3050, 3100, and 3160 cm^{-1}. Since common transitions are found for clusters based on the same amide but not for clusters having the same solvent bridges, coupling of the amide NH stretch to the unique set of mixed aromatic and aliphatic CH bend/NH bend overtones appears to be the most likely source of the Fermi resonance interaction. Additional support for this conclusion is provided by the RIDIR spectrum of the cyclic oxindole dimer[38] (not shown), which also displays a complex pattern of broadened peaks in the NH stretch region at the same frequencies as those found in OI−A_2 and OI−A_1W_1. Here, too, the amide NH stretch appears to have shifted to a sufficiently low frequency that the same 2:1 Fermi resonance interaction with the NH/CH bending modes of OI is operative.

In the presence of such strong Fermi resonance mixing, it is no longer possible to identify a distinct amide NH stretch fundamental. By comparison to spectra in which an amide NH stretch can be identified (such as in those of OI−A_1 or DQ−A_1), one concludes that its uncoupled frequency in the *cis*-amide−A_2 or *cis*-amide−A_1W_1(I) cluster must be shifted well below 3200 cm^{-1} for this interaction to occur. Shifts of this magnitude are exactly what the full DFT normal mode calculations yield for OI−A_2 and OI−A_1W_1(I) where the amide NH stretch is predicted to occur at 3053 and 3041 cm^{-1}, respectively. The strong, Fermi resonant mixing of the amide NH stretch observed in this work could be a quite general phenomenon, providing a characteristic spectral signature of strong hydrogen bonding to the *cis* amide group.

Acknowledgment. The authors gratefully acknowledge the support of the National Science Foundation (Grants CHE-9727527 and CHE-9728636) for this research.

References and Notes

(1) Olthof, E. H. T.; van der Avoird, A.; Wormer, P. E. S. *J. Chem. Phys.* **1994**, *101*, 8430.
(2) Nelson, D. D.; Fraser, G. T.; Klemperer, W. *J. Chem. Phys.* **1985**, *83*, 6201.
(3) Lee, J. S.; Park, S. Y. *J. Chem. Phys.* **2000**, *112*, 230.
(4) Sadlej, J.; Moszynski, R.; Dobrowolski, J. C.; Mazurek, A. P. *J. Phys. Chem. A* **1999**, *103*, 8528.
(5) Nimlos, M. R.; Kelley, D. F.; Bernstein, E. R. *J. Phys. Chem.* **1989**, *93*, 643.
(6) Held, A.; Pratt, D. W. *J. Am. Chem. Soc.* **1993**, *115*, 9718.
(7) Fedorov, A. V.; Cable, J. R. In preparation.
(8) Carney, J. R.; Fedorov, A. V.; Cable, J. R.; Zwier, T. S. *J. Phys. Chem. A* **2001**, *105*, 3487.
(9) Gotch, A. J.; Zwier, T. S. *J. Chem. Phys.* **1992**, *96*, 2496.
(10) Pribble, R. N.; Garret, A. W.; Haber, K.; Zwier, T. S. *J. Chem. Phys.* **1995**, *103*, 531.
(11) Becke, A. D. *J. Chem. Phys.* **1993**, *98*, 5648.
(12) Lee, C.; Yang, W.; Parr, R. G. *Phys. Rev. B* **1988**, *37*, 785.
(13) Frisch, M. J.; Pople, J. A.; Binkley, J. S. *J. Chem. Phys.* **1984**, *80*, 3265.
(14) Boys, S. F.; Bernardi, F. *Mol. Phys.* **1970**, *19*, 553.
(15) Frisch, M. J.; Trucks, G. W.; Schlegel, H. B.; Scuseria, G. E.; Robb, M. A.; Cheeseman, J. R.; Zakrzewski, V. G.; Montgomery, J. A., Jr.; Stratmann, R. E.; Burant, J. C.; Dapprich, S.; Millam, J. M.; Daniels, A. D.; Kudin, K. N.; Strain, M. C.; Farkas, O.; Tomasi, J.; Barone, V.; Cossi,

M.; Cammi, R.; Mennucci, B.; Pomelli, C.; Adamo, C.; Clifford, S.; Ochterski, J.; Petersson, G. A.; Ayala, P. Y.; Cui, Q.; Morokuma, K.; Malick, D. K.; Rabuck, A. D.; Raghavachari, K.; Foresman, J. B.; Cioslowski, J.; Ortiz, J. V.; Stefanov, B. B.; Liu, G.; Liashenko, A.; Piskorz, P.; Komaromi, I.; Gomperts, R.; Martin, R. L.; Fox, D. J.; Keith, T.; Al-Laham, M. A.; Peng, C. Y.; Nanayakkara, A.; Gonzalez, C.; Challacombe, M.; Gill, P. M. W.; Johnson, B. G.; Chen, W.; Wong, M. W.; Andres, J. L.; Head-Gordon, M.; Replogle, E. S.; Pople, J. A. *Gaussian 98*, revision A.7; Gaussian, Inc.: Pittsburgh, PA, 1998.

(16) Guelachvili, G.; Abdullah, A. H.; Tu, N.; Rao, K. N.; Urban, S. *J. Mol. Spectrosc.* **1989**, *133*, 345.

(17) Fedorov, A. V.; Cable, J. R. *J. Phys. Chem. A* **2000**, *104*, 4943.

(18) Robertson, E. G. *Chem. Phys. Lett.* **2000**, *325*, 299.

(19) Pimentel, G. C.; McClellan, A. L. *The Hydrogen Bond*; Freeman: San Francisco, 1960.

(20) Kleiner, I.; Brown, L. R.; Tarrago, G.; Kou, Q.-L.; Picqué, N.; Guelachvili, G.; Dana, V.; Mandin, J.-Y. *J. Mol. Spectrosc.* **1999**, *193*, 46.

(21) Iwasaki, A.; Fujii, A.; Watanabe, T.; Ebata, T.; Mikami, M. *J. Phys. Chem.* **1996**, *100*, 16053.

(22) Gotch, A. J.; Zwier, T. S. *J. Chem. Phys.* **1992**, *96*, 3402.

(23) Engdahl, A.; Nelander, B. *J. Chem. Phys.* **1989**, *91*, 6604.

(24) Frost, R. K.; Hagemeister, F. C.; Arrington, C. A.; Schleppenbach, D.; Zwier, T. S.; Jordan, K. D. *J. Chem. Phys.* **1996**, *105*, 2605.

(25) Del Bene, J. E. *J. Am. Chem. Soc.* **1995**, *117*, 1607.

(26) Dkhissi, A.; Adamowicz, L.; Maes, G. *J. Phys. Chem. A* **2000**, *104*, 5625.

(27) Stockman, A. P.; Bumgartner, R. E.; Suzuki, S.; Blake, J. A. *J. Chem. Phys.* **1992**, *96*, 2496.

(28) Masella, M.; Flament, J.-P. *J. Chem. Phys.* **1999**, *110*, 7245.

(29) Stepanov, B. *Nature* **1946**, *157*, 808.

(30) Sheppard, N. In *Hydrogen Bonding*; Hadzi, D., Ed.; Pergamon: New York, 1959.

(31) Leviel, J. L.; Marechal, Y. *J. Chem. Phys.* **1971**, *54*, 1104.

(32) Bratos, S. *J. Chem. Phys.* **1975**, *63*, 3499.

(33) Lassegues, J. C.; Lascombe, J. In *Vibrational Spectra and Structure*; Durig, J. R., Ed.; Elsevier: Amsterdam, 1982.

(34) Bratos, S.; Ratajczak, H.; Viot, P. In *Hydrogen-Bonded Liquids*; Dore, J. C., Teixeira, J., Eds.; Kluwer: Dordrecht, 1991.

(35) Henri-Rousseau, O.; Blaise, P. *Adv. Chem. Phys.* **1998**, *103*, 1.

(36) Henri-Rousseau, O.; Blaise, P. *Chem. Phys.* **1999**, *250*, 249.

(37) Chamma, D.; Henri-Rousseau, O. *Chem. Phys.* **1999**, *248*, 53.

(38) Florio, G. M.; Sibert, E. L., III; Zwier, T. S. *Faraday Discuss.* In press.